Structural Models of Human Big Conductance Calcium- and Voltage-gated Potassium Channels

Agata Kranjc [a], Claudio Anselmi [a], Paolo Carloni [a,b,c,*], Frank E. Blaney [d]

[a] *International School for Advanced Studies (SISSA/ISAS), Via Beirut 2-4, I-34014 Trieste, Italy*

[b] *CNR-INFM-DEMOCRITOS Modeling Center for Research in Atomistic Simulation, Via Beirut 2-4, I-34014 Trieste, Italy*

[c] *Italian Institute of Technology (IIT), SISSA-Unit, Via Beirut 2-4, I-34014 Trieste, Italy*

[d] *GlaxoSmithKline Pharmaceuticals, New Frontiers Science Park North, 3rd Avenue, Harlow, Essex CM19 5AW, UK*

Abstract

Human big conductance Ca^{2+}- and voltage-gated K^+ channels (hBK) are putative drug targets for cardiovascular, respiratory and urological diseases. Here we have used molecular simulation and bioinformatics approaches to construct models of two domains important for Ca^{2+} binding and channel gating, namely the regulator of conductance for K^+ (RCK1) domain and the so-called calcium bowl (CB). As templates for RCK1 were used the corresponding domains from a K^+ channel from *E. coli* and the K^+ channel from *Methanobacterium thermoautothropicum* (MthK). CB was modelled upon the structure of the human thrombospondin-1 C-terminal fragment and allowing the domain to relax in a simulated aqueous environment for 10-ns molecular dynamics simulations. The relevance of these models for interpreting the available molecular biology data is then discussed.

Key words: human big conductance calcium- and voltage-gated potassium channel (hBK); RCK1 domain (Regulate the Conductance of K^+); calcium bowl (CB); homology modeling; molecular dynamics (MD)

1. Introduction

Ca^{2+}- and voltage-gated big conductance K^+ channels (BK channels) are expressed by a variety of eukaryotic organisms. In mammals, they play an important role in muscle contractions, neuronal excitability, hormones and neurotransmitters release [1]. They are putative targets for pharmaceutical intervention for a variety of diseases, including cardiovascular, respiratory, urological diseases along with idiopathic epilepsy and ischemic reperfusion injury [2,3].

BK channels open upon an increase of intracellular Ca^{2+} ions (up to a concentration spanning 0.5 μM-50 mM [4]) along with an increase in the membrane electric potential [5]. Molecular biological experiments have established that these channels are homotetramers [6], composed of either α or α and β subunits along with four cytoplasmic domains: RCK1 and RCK2 (Regulate the Conductance of K+), the Ca^{2+}-binding domain, the so-called "calcium bowl" (CB) and the serine proteinase-like domain (SPLD) (Fig.1). The transmembrane region of the α subunit includes the S4 helix as the voltage sensor responsible for voltage sensitivity [7], the pore region through which K^+ ions flow out of the cell [8] and the S0 helix (present only in this channel) that places the N-terminus outside the cell [9]. Ca^{2+} ions are bound to the cytoplasmic domains: Ca^{2+} binding to two putative Ca^{2+}-binding sites in the RCK1 domain causes the gating of the channel [4,10,11]. A linker then connects RCK1 to RCK2, which is also important for the gating [12]. Finally,

* Corresponding author.
Email address: carloni@sissa.it (Paolo Carloni).

a CB domain is present. Mutations in this domain reduce the ability of low concentration of Ca^{2+} to activate the channel [13].

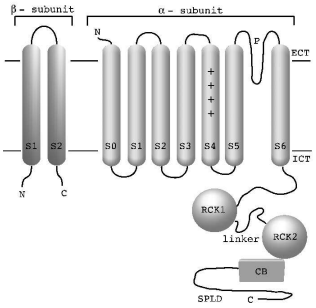

Fig. 1. All hBK channel monomers feature one subunit, which consists of a transmembrane domain (seven transmembrane-helix bundle and a pore helix), the RCK1, the linker and the RCK2 domains, the calcium-bowl and the SPLD domain [16]. Beside α subunit also β transmembrane subunit can be present, for which four different subtypes are known [14]. The most studied one (β1), shown here, is present in BK channels expressed in smooth muscles [15,16].

Besides the α subunit, there is also a β subunit (Fig.1) [6], which exists in four different subtypes, β1-β4 [14]. The most studied one is the β1 subunit in smooth muscle BK channels [15,16]. The β1 subunit increases Ca^{2+} sensitivity and decreases voltage sensitivity of BK channels [16].

Most of the drugs targeting the protein are believed to bind to the α subunit cytoplasmic domain, affecting Ca^{2+} affinity and modulating the interaction with the β subunits [2]. Few ligands interact with the transmembrane domain [2]. Therefore, structural information of both the transmembrane and cytoplasmic domains of the α subunit would be of great help for the rational design of ligands with large affinity for the channel. Unfortunately, such information is still lacking.

Here we have used bioinformatic, along with molecular dynamic, approaches to construct structural models for some of these domains. The available molecular biological data for the channel (see Supplementary Material) have been used to validate models of two of the channel domains. Firstly, the RCK1 domain, employing as templates the correspondent domains of two structurally similar channels: a K^+ channel from E.coli (PDB entry: 1ID1) [17] and the K^+ channel from *Methanobacterium thermoautothropicum* (MthK) (PDB entry: 1LNQ) [12] (it is worth noting that the latter is Ca^{2+}- (and not voltage-) gated). Secondly, the CB domain was modelled using a two stage strategy as the sequence analysis *per se* does not allow identifying the metal binding site(s). For this domain, we first modelled the CB, using as the template one of the Ca^{2+}-binding domains from human thrombospondin-1 C-terminal fragment (PDB entry: 1UX6, from A865 to N897) [18], and we then attempt to identify the metal binding sites by performing molecular dynamics (MD) simulations with Ca^{2+} ions placed in five different locations, these are referred to for clarity as Ca1-Ca5. No attempts are made to construct tetrameric structures and only isolated RCK1 and CB domains were considered. The way the subunits assemble is indeed not known and there are no experiments involving the subunit-subunit interface, which could help assisting the modelling of the quaternary structure of the protein.

In addition, for the transmembrane region and RCK2, although there are reasonably good templates (*e.g.* voltage-gated K^+ channel K_v1.2 [19], *E. coli* K^+ channel [17], MthK [12]), molecular biology data are not available. Therefore we limit the analysis for these domains to the sequence alignment. For the linker and SPLD, there are not reliable templates presently and they are not investigated here.

2. Methods

We have used Standard bioinformatics and Molecular simulation protocols, which are described in the Appendix A.

3. Results

The alignment for the **transmembrane region** S0-S3 with K_v1.2 turned out to exhibit large gaps, together with the two missing parts (36 and 12 amino acids) in the structure of K_v1.2; as a result, we restricted our analysis to the S4-S6 tract (Fig.2). The sequence identity for the region from S4-S6 between hBK and K_v1.2 is 21%, while the homology for the same part is 50% (Fig.2).

The following features can be noticed: (i) as expected the GYG fingerprint, highly conserved signature among K^+ channels [20] is located in the selectivity filter. It is responsible for the high selectivity of K^+ over Na^+. (ii) In general, K_v channels have conserved PXP sequence as the gating hinge in the last part of S6 helix [21]. In hBK is conserved just one proline (P385), which could cause breaks or irregularities in the helix structure and can be there-

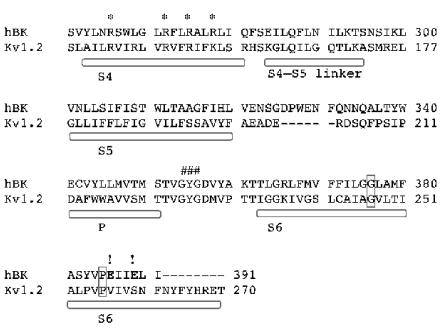

Fig. 2. Alignment between S4-S6 region of hBK and $K_v1.2$ channel. Structurally and functionally important features are shown: (i) positively charged residues in S4, which constitute the voltage sensor are labeled by stars (*); (ii) GYG as the fingerprint of selectivity filter is signed by hashes (#) [20]; (iii) G376 and P385 as putative gating hinges in hBK are depicted by boxes (iv) E386 & E389 that form the ring of negatively charged residues [8] are denoted with the exclamation mark (!).

fore considered as putative gating hinge. However, also G376 in S6 helix, which is conserved among K^+ channels and corresponds to G83 in MthK [22] and to G247 in $K_v1.2$ [19] could be a good candidate for the hinge. (iii) The S4 helix with its repeats of positively charged residues (Arg) followed by two hydrophobic residues represents the voltage sensor [7]. In comparison with $K_v1.2$, hBK lacks two positively charged residues. (iv) Two adjacent rings of four Glu residues are positioned at the entrance of the intracellular vestibule [8]. These eight Glu's play a key role for the high conductance of the channel by attracting intracellular K^+ ions, concentrated at the entrance of the intracellular vestibule. In fact, Glu to Gln mutation in either ring decreases single channel current by about 12 pA, whilst the mutation of all the eight Glu's in the ring cause the conversion to an inwardly rectifying channel [8].

The **RCK1 domain** starts at the highly conserved ^{409}HIVVC [17] and finishes at FSMRS^{580} (Fig.3A). Its fold is the Rossmann fold with two additional helices (Fig.3B) [17]. The model includes the salt bridge formed by K513 and D546 (Fig.3C) as established by molecular biological experiments [17], which show that mutations K513D or D546K reduce open probability of the channel. This salt bridge has to be considered as an input in the model, as it does not emerge from the alignment procedure only.

Two putative Ca^{2+}-binding sites have been identified [4,10,11]. One is formed by D427 and D432 which binds Ca^{2+} in concentrations at around

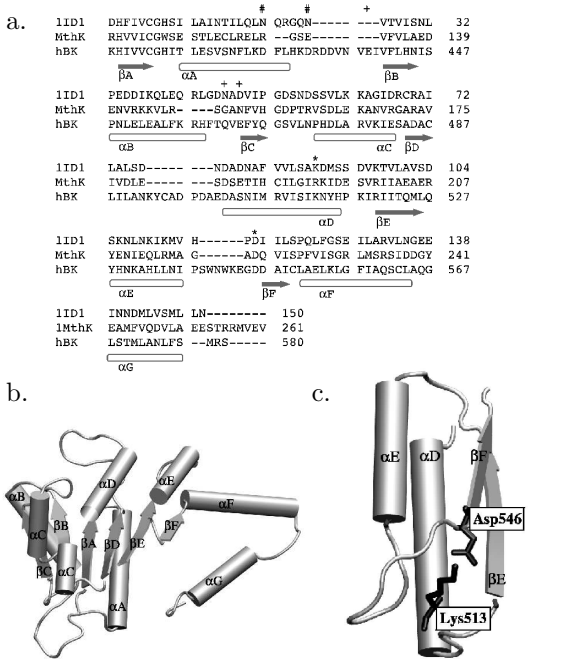

Fig. 3. A: Alignment of the two RCK domains from *E. coli* and MthK with the corresponding sequence in hBK. The following features are shown using hBK notation: (i) salt bridge formed by K513 and D546 is labeled by stars (*); (ii) putative high affinity Ca^{2+}-binding site [4,11] composed by D427 and D432 is depicted by hashes (#); (iii) putative low affinity Ca^{2+}-binding site [4,10,11], constructed by E439, Q462 and E464, is denoted with plus signs (+). B: The model of the RCK1 domain. C: Salt bridge formed by K513 and D546 was included in the model and is consistent with the molecular biology data [17].

10 μM. In fact, D432A produces a marked reduction in the ability of Ca^{2+} to shift gating, while D427A mutation exhibits the same behaviour as the wild type channel [4]. In order to identify such binding sites, we scanned a set of Ca^{2+}-binding proteins from the PDB database. In general Ca^{2+}-binding sites involve three to four negatively charged residues (see Supplementary Material), each contributing with either one or both oxygen atoms. In addition, as Ca^{2+} is usually coordinated with 6-8 oxygen atoms [23] (see Supplementary Material), water and/or oxygen atoms from the backbone or the side chains of Gln and/or Asn could contribute to the binding. Therefore, in the high affinity binding site, beside the suggested D427 and D432, D434 and/or D435 may also bind Ca^{2+}. The model supports that D427 and D432 do not bind to the metal ion, although this has not been firmly established yet.

The **calcium bowl (CB)** is a crucial domain

for Ca^{2+} binding [11,24,25]. Molecular biological experiments show that there are five adjacent Asp's residues (D959-D963 in the sequence: ^{945}TELV...DQ DDDDDPD...CGTA^{979}), which most probably bind the metal ions [24,25]. Beside them, there are other oxygen-containing residues, which can coordinate Ca^{2+} as well (Fig.4A) [24,25]. The model can be formally divided in two segments, one formed by 17 (T945-D961) and the other by 18 (D962-A979) residues. An α-helix is present in the first segment, the rest forms a coil. Each segment bears two Ca^{2+}-binding sites (Ca1, Ca2 and Ca3, Ca4), whereas the fifth one (Ca5) is in between. Unfortunately, there are no templates sharing high sequence identity with CB, furthermore the number of calcium ions binding to it is unknown. The best template for this domain, the human thrombospondin-1 C-terminal fragment (Fig.4A [18]) exhibits SI=17% and SH=43%. Therefore we decided to construct first a model based on such template (namely from T945 to A979) and then to relax it by NPT MD simulations in aqueous solution. The five Ca^{2+} in the template were added in the corresponding binding sites of the model (Ca1-Ca5) in order to verify if they remained in these positions during the MD simulation. Obviously, the exact number and the coordination of Ca^{2+} bound to the CB have to be validated against further biochemical experiments.

At the end of the MD run (10 ns), the model structure from T945 to E967 keeps the fold similar to the initial one (Fig.4B), while the part from L968 to A979 is unfolded. Ca^{2+}-binding sites are present in the structured part of the CB model. Four Ca^{2+} ions (in the position of Ca1-Ca4) maintain their coordination and are hereafter described (Fig.4C): (i) Ca1 is bound by D959, D961, D963 and E967 carboxyl oxygen atoms along with D963, D965 backbone oxygen and one water molecule. (ii) D961, D963, and E967 coordinate with their second carboxyl oxygen atoms the neighbouring Ca2. Beside them, Ca2 is bound also with D965 and three water molecules. (iii) Ca3 is bound by D950, D957 and D962 carboxyl oxygen atoms beside the D959 backbone oxygen and three waters. (iv) The neighbouring Ca4 is also bound by D950 and D957 carboxyl oxygen atoms along with E946 carboxylate group, N952 backbone oxygen and four water molecules. (v) In contrast, one Ca^{2+} ion (Ca5) is mostly coordinated by the solvent. The protein ligands are D960 side chain and Q954 backbone carbonyl. Its dissociation, observed after ≈9.6 ns, may be caused by the fact that in the initial model Ca5 is bonded to a

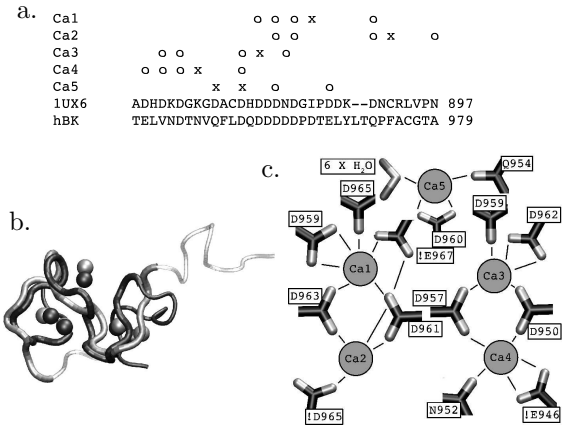

Fig. 4. A: Alignment between human Thrombospondin-1 and hBK Ca^{2+}-binding domain (CB). Residues in the template binding Ca^{2+} ions with the side chain are depicted with the circle 'o'; those binding Ca^{2+} with the backbone oxygen with 'x'. B: Superimposition of the initial structure of the model (black) and the structure after 10 ns of MD simulations (gray). Spheres represent Ca^{2+} ions. C: Putative Ca^{2+}-binding sites in the CB model after 10-ns MD simulations. Note that Ca5 is not coordinated with enough oxygens and is therefore not considered as a Ca^{2+}-binding site, but is shown here as the final result. Residues depicted with an exclamation mark (!) do not bind Ca^{2+} in the initial model of CB. Water molecules that coordinate Ca^{2+} ions, Ca1-Ca4, and D963 backbone oxygen which binds Ca1 are not shown due to clarity's sake.

smaller number of protein ligands than Ca1-Ca4.

Our MD model appears to be consistent with most experimental data (see Supplementary Material): the five adjacent Asp's (D959-D963) in the core of CB are reported as important for Ca^{2+} sensitivity and/or binding [24] and in our model four of them (D959, D961, D962 and D963) coordinate Ca^{2+}. (ii) N949, N952 and Q954 are reported not to coordinate Ca^{2+} with their side chain oxygen atoms [24,25], this is fully consistent with our model. (iii) Q958 and Q972 do not bind Ca^{2+}, which is consistent with the results obtained in the study by Bao *et al.* [24]. (iv) In addition, the finding that E946 and D957 bind Ca^{2+} is fully consistent with the data obtained by Sheng *et al.* [25], where they have shown that single or combined mutations of E946A and D957A reduces Ca^{2+} sensitivity and binding. However, it should be mentioned that it has been reported elsewhere [24] that both Glu's present in the CB are not important for Ca^{2+} binding, in contrast to the previous study. This issue therefore requires further studies. (v) The fact that D960 plays a role for Ca^{2+} sensitivity and binding [24] may be also consistent with our model. Although in our structure, Ca5 is

not directly bound to D960, the negative electrostatic potential of the latter may play a very important role for stabilizing the ion in the close proximity of the protein (Fig.4C).

The model is not consistent with some experimental data. Firstly, mutations of D950 and D965 to Ala do not influence Ca^{2+} sensitivity or binding [24,25], yet in our model D950 and D965 bind Ca3, Ca4 and Ca2, respectively. In addition, E967 should not bind Ca^{2+}[24], yet in our model it does bind Ca1 and Ca2. More refined models could take these pieces of information into account by performing constraint molecular dynamics simulations.

In conclusions, we have used biocomputing techniques to provide structural insights into the human big conductance Ca^{2+}- and voltage-gated K^+ channel. We constructed a model of the RCK1 domain, which exhibits the template Rossmann fold with two additional helices and one for the calcium bowl. These models explain most of the available data and can be helpful for planning future molecular biology experiments in this pharmacologically relevant channels.

Acknowledgements

This work was supported by GlaxoSmithKline (GSK), Stevenage, UK. We thank Anna-Maria M. Capelli, Aldo G. Feriani and Iain M. Mclay, Alejandro Giorgetti and Janez Mavri for many stimulating discussions.

Appendix A. Method

A.1. *Transmembrane region*

hBK transmembrane region sequence was aligned to that of $K_v1.2$ (PDB entry: 2A79) [19] using the ClustalW program [26].

A.2. *RCK1*

Two templates were found: the RCK domains in an *E. coli* K+ channel (PDB entry: 1ID1) [17], which form a dimer, and those of the MthK channel (PDB entry: 1LNQ) [12], which construct a dimer of dimers. Both share with RCK1 18% of sequence identity (SI) and 40% of sequence homology (SH).

We first performed a structural alignment between the RCK domains from MthK and *E. coli* by using Swiss-Pdb Viewer 3.7 [27]. Then we performed the sequence alignment of RCK1 from hBK against both templates, using the same program. Gaps were manually removed from the secondary structure element sequence tracts. 3-D models were eventually built using MODELLER 6v2 [28]. A distance restraint between NZ@K513 and CG@D546 atoms was included in the model in order to form a salt bridge, whose presence has been suggested by experiments [17].

A.3. *Calcium bowl (CB)*

The best template for CB is the 35 residues long segment of the human thrombospondin-1 C-terminal fragment (PDB entry: 1UX6, from A865 to N897, SI=17%, SH=43%, Fig.5A) [18], as shown by a Blast [29] search. It binds five Ca^{2+} ions; therefore five Ca^{2+} ions were added to the 3-D model of CB, built as above with MODELLER 6v2 [28], with similar coordination as in the template. The resulting adduct was inserted in a box of dimensions 46 x 46 x 46 $\AA$ packed with 3955 water molecules. The system underwent MD simulations using the Gromacs-3.2.1 program [30]. The Amber parm99 [31] and TIP3P [32] force fields were used for the protein frame with the metal ions and the solvent, respectively. The model was initially minimized with positional restraints on the solute with a stepwise (each 100 ps) reduced force constant from 1000 kJ mol^{-1} nm^{-2} till 0 kJ mol^{-1} nm^{-2} (in steps of 200 kJ mol^{-1} nm^{-2}). After, an unconstraint MD was carried out for an overall length of 10 ns. A time step of 2 fs was used. All bond lengths were kept fixed applying the LINCS algorithm [33]. Temperature (300 K) and pressure (1 bar) were kept constant by coupling the system to a few Berendsen thermostats [34]. Periodic boundary conditions were applied treating long-range electrostatic interactions with the particle-mesh Ewald technique using a cut-off of 10 $\AA$ for the real part of the electrostatic. The same cut-off was used for the van der Waals interactions. Pair lists were updated every 20 steps.

A.4. *RCK2, linker, SPLD*

For RCK2 domain, the low sequence identity (15% or less) with other domains with known structure (*i.e. E. coli* K+ channel [17] and MthK [12]) and the absence of biological data prevented 3-D mod-

elling and sequence analyses. For the linker region, there are well conserved parts (up to 30 residues out of 200), but the presence of very large gaps (more than 15 residues) does not allow more straightforward analyses. Finally, we could not identify any good template for the SPLD domain.

References

[1] A. Wickenden, Pharmacol. Ther. 94 (2002) 157.

[2] S. Ghatta, D. Nimmagadda, X. Xu, S. T. O'Rourke, Pharmacol. Ther. 110 (2006) 103.

[3] V. Calderone, Curr. Med. Chem. 9 (2002) 1385.

[4] X. M. Xia, X. Zeng, C. J. Lingle, Nature 418 (2002) 880.

[5] B. S. Pallotta, J. Gen. Physiol. 86 (1985) 601.

[6] M. Garcia-Calvo, H. G. Knaus, O. B. McManus, K. M. Giangiacomo, G. J. Kaczorowski, M. L. Garcia, J. Biol. Chem. 269 (1994) 676.

[7] L. Diaz, P. Meera, J. Amigo, E. Stefani, O. Alvarez, L. Toro, R. Latorre, J. Biol. Chem. 273 (1998) 32430.

[8] T. I. Brelidze, X. Niu, K. L. Magleby, Proc. Natl. Acad. Sci. U. S. A. 100 (2003) 9017.

[9] P. Meera, M. Wallner, M. Song, L. Toro, *Proc. Natl. Acad. Sci. U. S. A.* **94** (1997) 14066.

[10] J. Shi, G. Krishnamoorthy, Y. Yang, L. Hu, N. Chaturvedi, D. Harilal, J. Qin, J. Cui, Nature 418 (2002) 876.

[11] X. H. Zeng, X. M. Xia, C. J. Lingle, J. Gen. Physiol. 125 (2005) 273.

[12] Y. Jiang, A. Lee, J. Chen, M. Cadene, B. T. Chait, R. MacKinnon, Nature 417 (2002) 515.

[13] M. Schreiber, L. Salkoff, Biophys. J. 73 (1997) 1355.

[14] P. Orio, P. Rojas, G. Ferreira, R. Latorre, News Physiol. Sci. 17 (2002) 156.

[15] X. Qian, C. M. Nimigean, X. Niu, B. L. Moss, K. L. Magleby, J. Gen. Physiol. 120 (2002) 829.

[16] L. Bao, D. H. Cox, J. Gen. Physiol. 126 (2005) 393.

[17] Y. Jiang, A. Pico, M. Cadene, B. T. Chait, R. MacKinnon, Neuron 29 (2001) 593.

[18] M. Kvansakul, J. C. Adams, E. Hohenester, EMBO J. 23 (2004) 1223.

[19] S. B. Long, E. B. Campbell, R. MacKinnon, Science 309 (2005) 897. In that 903

[20] D. A. Doyle, C. J. Morais, R. A. Pfuetzner, A. Kuo, J. M. Gulbis, S. L. Cohen, B. T. Chait, R. MacKinnon, Science 280 (1998) 69.

[21] a) N. Ottschytsch, A. Raes, D. Van Hoorick, D. J. Snyders, Proc. Natl. Acad. Sci. U. S. A. 99 (2002) 7986. b) T. Harris, A. R. Graber, M. Covarrubias, Am. J. Physiol. Cell Physiol. 285 (2003) C788-C796. c) D. Kerschensteiner, F. Monje, M. Stocker, J. Biol. Chem. 278 (2003) 18154. (d) A. J. Labro, A. L. Raes, I. Bellens, N. Ottschytsch, D. J. Snyders, J. Biol. Chem. 278 (2003) 50724. (e) N. Ottschytsch, A. L. Raes, J. P. Timmermans, D. J. Snyders, J. Physiol. 568 (2005) 737.

[22] Y. Jiang, A. Lee, J. Chen, M. Cadene, B. T. Chait, R. MacKinnon, Nature 417 (2002) 523.

[23] J. K. Jaiswal, J. Biosci. 26 (2001) 357.

[24] L. Bao, C. Kaldany, E. C. Holmstrand, D. H. Cox, J. Gen. Physiol. 123 (2004) 475.

[25] J. Z. Sheng, A. Weljie, L. Sy, S. Ling, H. J. Vogel, A. P. Braun, Biophys. J. 89 (2005) 3079.

[26] J. D. Thompson, D. G. Higgins, T. J. Gibson, Nucleic Acids Res. 22 (1994) 4673.

[27] N. Guex, M. C. Peitsch, Electrophoresis 18 (1997) 2714.

[28] A. Šali, T. L. Blundell, J. Mol. Biol. 234 (1993) 779.

[29] S. F. Altschul, W. Gish, W. Miller, E. W. Myers, D. J. Lipman, J. Mol. Biol. 215 (1990) 403.

[30] D. van der Spoel, E. Lindahl, B. Hess, A. R. van Buuren, E. Apol, P. J. Meulenhoff, D. P. Tieleman, A. L. T. M. Sijbers, K. A. Feenstra, R. van Drunen, H. J. C. Berendsen, in *Gromacs User Manual version 3.2* (2004).

[31] J. W. Ponder, D. A. Case, Adv. Protein Chem. 66 (2003) 27.

[32] W. L. Jorgensen, J. Chandrasekhar, J. D. Madura, R. W. Impey, M. L. Klein, J. Chem. Phys. 79 (1983) 926.

[33] B. Hess, H. Bekker, H. J. C. Berendsen, J. G. E. M. Fraaije, J. Comp. Chem. 18 (1997) 1463.

[34] H. J. C. Berendsen, J. P. M. Postma, W. F. van Gunsteren, A. Di Nola, J. R. Haak, J. Chem. Phys. 81 (1984) 3684.

[35] F. C. Berenstein, T. F. Koetzle, G. J. Williams, E. F. Meyer, Jr., M. D. Brice, J. R. Rodgers, O.Kennard, T. Shimanouchi, M. Tasumi, J. Mol. Biol. 112 (1977) 535.

mutations	*experiment*	*model*	*model* − 10*ns*
E946A	no changes [24]; reduces Ca^{2+} sensitivity and binding (30%)	does not bind Ca^{2+}	4[2ox]
N949A	no change [24]	does not bind Ca^{2+}	does not bind Ca^{2+}
D950A	no change [25]	3[1ox]; 4[1ox]	3[1ox]; 4[1ox]
N952A	no change [24,25]	4[bb ox]	4[bb ox]
Q954A	no change [24,25]	5[bb ox]	5[bb ox]
D957A	reduces Ca^{2+} sensitivity (50%) and Ca^{2+} binding (30%) [24,25]	3[1ox]; 4[1ox]; 5[bb ox]	3[1ox]; 4[1ox]
Q958A	reduces Ca^{2+} sensitivity (50%) and binding (20%) [24]	does not bind Ca^{2+}	does not bind Ca^{2+}
D959A	reduces Ca^{2+} sensitivity (60%); no data for Ca^{2+} binding [24]	1[1ox]; 3[bb ox]	1[2ox]; 3[bb ox]
D960A	reduces Ca^{2+} sensitivity (90%) and binding (50%) [24]	5[2ox]	5[2ox]
D961A	no change in Ca^{2+} sensitivity; reduces Ca^{2+} binding (50%) [24]	1[1ox]; 2[1ox]	1[1ox]; 2[1ox]
D962A	reduces Ca^{2+} sensitivity (90%) and binding (50%) [24]	3[1ox]	3[2ox]
D963A	reduces Ca^{2+} sensitivity (40%); no data about binding [24]	1[1ox]; 2[1ox]	1[1ox,bb ox]; 2[1ox]
D965A	reduces Ca^{2+} binding (30%) [24]	1[bb ox]	1[bb ox]; 2[1ox]
E967A	no change [24]	does not bind Ca^{2+}	1[1ox]; 2[1ox]
Q972A	reduces Ca^{2+} sensitivity (40%); no data about binding [24]	does not bind Ca^{2+}	does not bind Ca^{2+}
E946A/D957A	reduces Ca^{2+} sensitivity and binding (60%) [25]		
D960A/D962A	reduces Ca^{2+} binding (80%) [24]		
D961A/D963A	reduces Ca^{2+} binding (75%) [24]		
K513D	cause upward shift in the Ca^{2+} activation profile [17]		
D546K	cause upward shift in the Ca^{2+} activation profile [17]		
K513D/D546K	shift in the Ca^{2+} activation profile similar to that of WT [17]		

Tab. 1. Avaliable experimental data from which structural information can be extracted. In the columns MODEL are presented results from homology model followed by the results of MD simulations of Ca^{2+} binding to the CB after 10 ns. Numbers 1, 2, 3, 4 and 5 identify position of each Ca^{2+} included inthe model and represent which Ca^{2+} binds to the determined residue; "bb ox" stands for backbone oxygen.

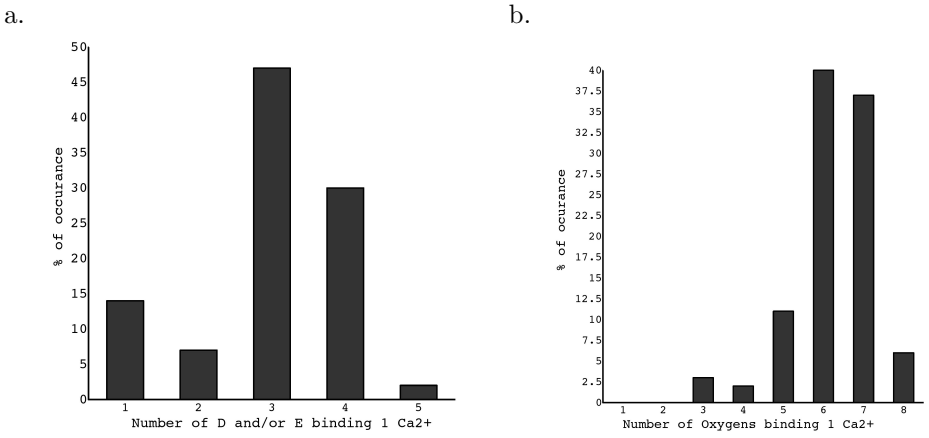

Fig. A.1. Number of negatively charged residues (Asp, Glu) (A) and oxygens (B) needed to bind one Ca^{2+} ion as determined by the analysis of 87 bonded Ca^{2+} ions in 20 Ca^{2+}-binding proteins from PDB database [35].